

Chapter 29

Exposure of Coastal Ecosystem Services to Natural Hazards in the Bangladesh Coast



Sanjoy Roy and Daniel Depellegrin

Significance Statement Knowledge about the impacts of natural hazards on ecosystem services is crucial to guide the effective management of ecosystem components in a particular landscape. The coastal landscape of Bangladesh is a source of numerous ecosystem services on one hand and also exposed to natural hazards, especially to tropical cyclones on the other hand. Almost every year the tropical cyclones and associated storm surges cause severe devastation to the ecosystem services in the eastern coastal region of the country. We for the very first time in Bangladesh applied the remote sensing method with the Millennium Assessment technique to map coastal ecosystem service capacity and assess their degree of exposure to the tropical cyclone in the eastern coastal region of the country. Our study identifies the aquatic environments, mangrove and hilly forests having the highest potentials of ecosystem service capacity, which needs to be protected from the natural hazards through implementing appropriate land use and nature-focused disaster management policies for sustainable, equitable, and effective use of the ecological resources.

Keywords Ecosystem services · Tropical cyclone · Remote sensing · Coastal Bangladesh · Ecosystem threats

1 Introduction

Extreme meteorological events, such as tropical storms, hurricanes, and cyclones can cause severe environmental degradation and damage to socio-economic assets (Meixler, 2017). Within these increasing threats also ecosystem services (ES) can be

S. Roy (✉)

Bengal Institute for Architecture, Landscapes and Settlements, Dhaka, Bangladesh

D. Depellegrin

Landscape Analysis and Management Laboratory, Department of Geography,
University of Girona, Girona, Spain

exposed to extreme events leading to ecosystem services loss, or temporary impairment of flow and use of the ES (Menegon et al., 2018). In the last decade, an increased amount of literature dealing with ES risk or damage assessment in the context of extreme events was produced. Moreover, the growing use of satellite-based remote sensing and geospatial techniques has brought significant advancement in the field of ES assessment throughout the globe. For instance, for the Indian Ocean Tsunami of 2004 Kaiser et al. (2013) applied remote sensing and GIS techniques to analyze coastal risk to ecological resources on the coast of Thailand. A study conducted by Meixler (2017) analyzed the ES loss caused by Hurricane Sandy in habitats within Jamaica Bay and New York using orthoimagery and land use maps. Another study successfully estimated specific ES loss and recovery in mangrove ecosystems through the assessment of the impacts of Hurricane Charley 2004 on the aboveground carbon stock in Southwest Florida (Peneva-Reed et al., 2020). Despite several pieces of literature on the ES assessment, there is little knowledge for the coast of Bangladesh.

Bangladesh is a coastal state exposed to the Bay of Bengal and is subjected to a number of natural and anthropogenic hazards, which cause substantial damage to the ES every year. Among different hazards, tropical cyclone causes severe damage to the ESs in coastal Bangladesh due to its intensity and recurrence nature.

The aim of this study is to analyze the ES capacity from remote-sensing based land use (LU) detection for the eastern coastal districts such as Chattogram and Cox's Bazar located in the south-east of Bangladesh. The threat to ES provided by LU units will be analyzed for a cyclone database from 1952 to 2017 and administrative units called *upazila* of highest ES loss/impairment will be defined and discussed.

2 Materials and Methods

2.1 Study Area Description

The study area includes the entire eastern coastal region of Bangladesh, which traverses Chattogram and Cox's Bazar districts (Fig. 29.1). Geographically it extends from $20^{\circ}35'17'' - 22^{\circ}59'28''$ N latitude to $91^{\circ}16'20'' - 92^{\circ}21'37''$ E longitude and covers 7113 km² area, approximately. This region is bounded by the Feni river to the north to Saint Martin's Island to the south and the Bay of Bengal to the west to Chattogram hill tract to the east, which is characterized by heterogeneous landscapes including coastal plain, sandy beaches, marshes, and hills of tertiary origin. Tropical monsoon climate characterized by high summer temperature ($\approx 32.3^{\circ}\text{C}$), high humidity, and sufficient rainfall during the monsoon (≈ 3000 mm) prevails in the study area (BMD, 2013; Roy et al., 2020). The hilly areas are covered by the semi-evergreen deciduous to tropical evergreen rain forests, whereas the extensive plain land is mostly dominated by different species of homestead vegetation. This region holds 10.16 million populations (BBS, 2011), where a significant

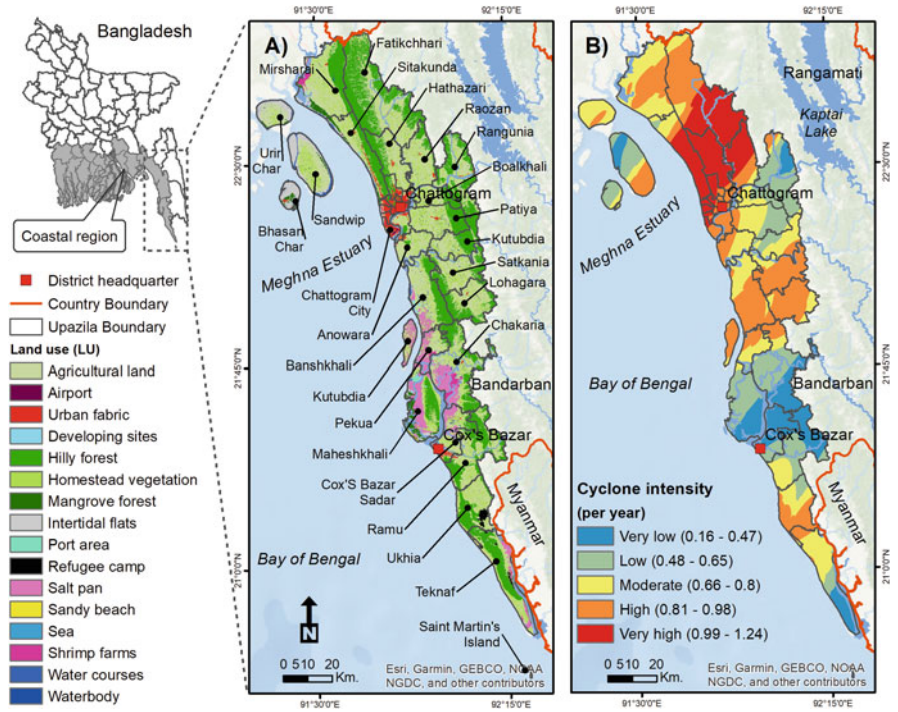


Fig. 29.1 Geographical setting and administrative units of the study area. (a) Land uses derived from Landsat 8 Operational Land Imager (OLI) satellite image-based remote sensing technique and (b) Cyclone intensity per year per 20 km radius calculated based on cyclone occurrences from 1952 to 2017

portion lives in Chattogram city, the largest port city and the major economic hub of the country. With a number of tourist spots and a 145 km long sandy beach, the longest sea beach in the world, this region is the major touristic part of the country. Diverse LU existed in the region are the sources of different ecosystem services and provide ample benefits to the inhabitants and the natural environment. Among several natural and anthropogenic hazards, this region is highly exposed to tropical cyclones and cyclone-induced storm surges (Hoque et al., 2019). Since 1952 approximately 34 catastrophic cyclones have made landfall in the region, which caused significant damage to ecosystem services with loss of lives and economic properties.

2.2 Extraction of LU Using Remote Sensing

Four cloud-free and near dated Landsat 8 Operational Land Imager (OLI) images were retrieved from the USGS global data hub (<https://earthexplorer.usgs.gov/>) for

Table 29.1 Properties of the satellite imagery and cyclone data used in the study

Dataset	Years of analysis	Sensor/sources	Image acquisition dates	Path/row	Spatial resolution
Satellite imagery	2020	Landsat 8 OLI	28-Jan-20	135/45	30 m (visual and infra-red spectral bands)
			28-Jan-20	135/46	
			19-Jan-20	136/44	
			19-Jan-20	136/45	
Tropical cyclone tracks	1952–2017	IBTrACS (International Best Track Archive for Climate Stewardship; http://ibtracs.unca.edu/)			
Cyclone wind speed (km/h)	1952–2017	National newspaper archive (Daily Ittefaq, Daily Prothom Alo, The Daily Star, Jugantor, and The Sangbad); Alam and Dominey-Howes (2014)			

extracting LU of the study area (Table 29.1). The images were subjected to atmospheric correction for obtaining surface reflectance with minimal atmospheric and aerosol effects. Given the higher accuracy, the Fast Line-of-sight Atmospheric Analysis of Spectral Hypercube (FLAASH) was applied to the images for correcting them atmospherically (Emran et al., 2018). FLAASH atmospheric correction module is the first-principles atmospheric correction modelling tool that starts with the conversion of image data to at sensor spectral radiance for obtaining surface reflectance through a set of equations (Emran et al., 2018; FLAASH User’s Guide, 2006). In the first stage of the atmospheric correction process, the Digital Numbers (DN) of the images were converted to the Top of Atmospheric Radiance (TOA) using the following standard equation (USGS, 2020).

$$L_{\lambda} = M_L Q_{cal} + A_L \quad (29.1)$$

Whereas, L_{λ} is the TOA spectral radiance, M_L is the band-specific multiplicative rescaling factor obtained from the image metadata, Q_{cal} is the quantized and calibrated pixel’s DN values, and A_L is the band-specific additive rescaling factor.

In the second stage, the FLAASH was applied over the TOA radiance images using the appropriate definition of aerosol model, image properties, Modtran Multiscatter model (FLAASH User’s Guide, 2006), and ground elevation. Finally, the output atmospherically corrected surface reflectance images were mosaiced together and used as an input in the LU extraction procedure.

In the study area, 11 dominant LU were identified which were extracted from the surface reflectance image through the hybrid image classification approach (Roy & Mahmood, 2016). In the image classification procedure, the image was first classified into 300 arbitrary classes based on the spectral responses of the pixels using the Iso Cluster Unsupervised algorithm. From these arbitrary classes, 20 spectral signatures for each LU category were selected and thus a set of training samples was developed. In the second stage, this training sample set was used in the Random Forest Supervised classification algorithm to extract the LU for the entire study area. A 3 * 3 median filter was further applied to reduce noise in the classified image. After

that, the waterbody was reclassified into three classes (i.e., waterbody, sea, and watercourse) and port areas (i.e., airport and seaport) and shrimp farms were manually defined in the classified LU image as these are difficult to distinguish from the spectral characters of the urban fabric and salt pan, respectively. Thus, 16 final LU categories were obtained from the satellite imagery (Fig. 29.1a), where the overall accuracy of the classification was obtained higher than 90%.

2.3 Calculation of Cyclone Intensity

Spatial tracks of the tropical cyclones that made landfall in the study area between 1952 and 2017 were obtained from the International Best Track Archive for Climate Stewardship (IBTrACS) database. Wind speeds of the corresponding cyclone tracks were collected from the national newspaper archive and Alam and Dominey-Howes (2014). We considered a 20 km radius circle from each track as the maximum impact area of the respective cyclone and thus developed a number of circles throughout the study area. Finally, the intensity of the cyclones in the study area was calculated (Fig. 29.1b) using the circle radius, track length that falls within the circle, and corresponding wind speed according to the following equation.

$$\text{Cyclone intensity (CI)} = \frac{\sum_{k=1}^{k=n} L_k \times W_k}{R_c} \quad (29.2)$$

Where, L_k is the length of cyclone track k that falls in the circle with 20 km radius, W_k is the wind speed of the cyclone track k , and R_c is the radius of the circle (20 km).

2.4 Assessing Ecosystem Services and Threat Exposure

Based on the LUs extracted through remote sensing technique an ES capacity analysis was performed using literature review and expert scoring. According to Villamagna et al. (2013) the ES capacity (ES_{Cap}) is defined as the potential of ecosystems to provide goods and services. A popular approach to analyze and map ES on large spatial scales is to link ES classifications, such as the Millennium Assessment (MA 2005) with LU components into an ES-LU matrix/look-up table (Campagne et al., 2020). The advantage of the ES-LU matrix approach is its applicability in different biomes, e.g., terrestrial (Müller et al., 2020) or coastal marine (Depellegrin et al., 2017), its ability to cover different spatial scales and its ease for communication to decision-makers and non-scientific stakeholders. In contrast to the archetypical ES-LU matrix (e.g., Burkhard et al., 2009) we represent the ES_{Cap} using an alluvial diagram (Fig. 29.2a). The alluvial diagram is organized into ES-ES Categories-LU paradigm that links the ES_{Cap} to the LU of the study area.

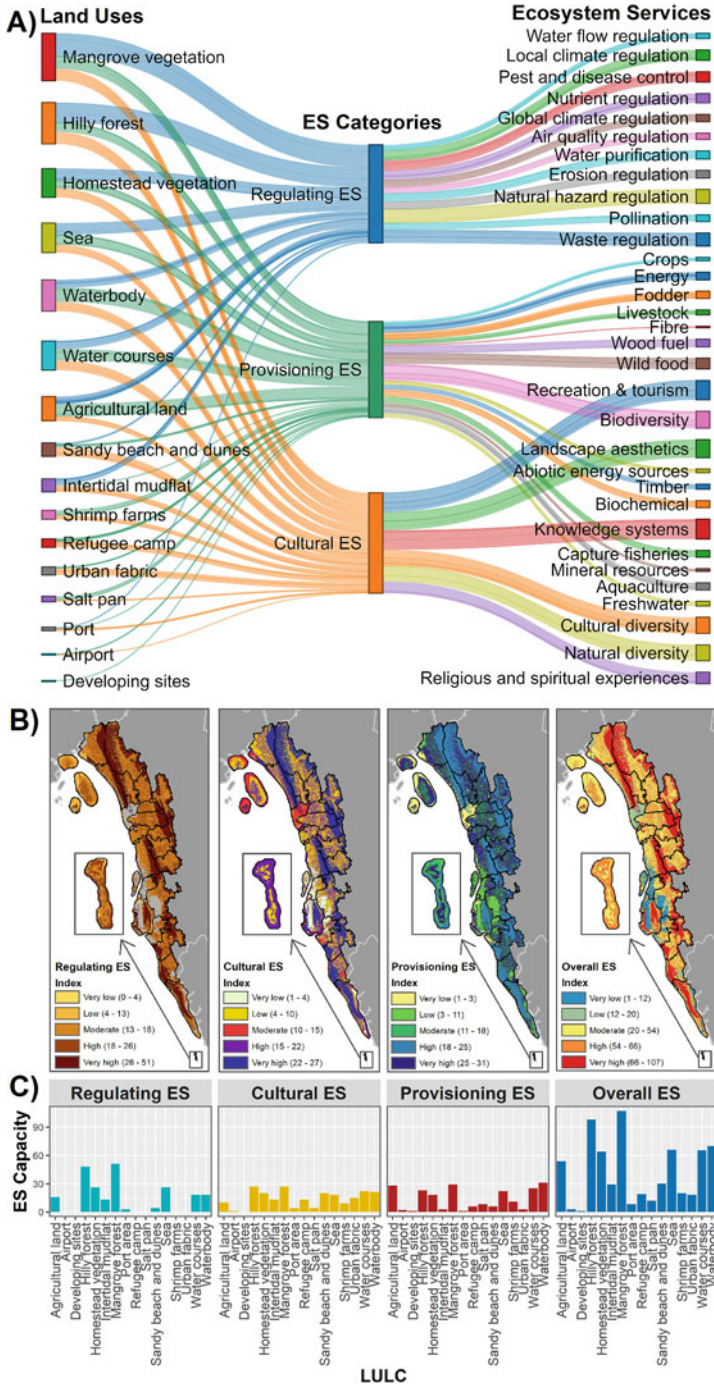


Fig. 29.2 (a) Alluvial diagram representing the ecosystem services identified, the ES categories, and the ES_{Cap} of different LU types to support ES provision. (b) Geographic distribution of Coastal Ecosystem Services Capacity; (c) Average contribution in % by LU to ES_{Cap}

The thickness of the flow bars corresponds to the ES_{Cap} scored from 1 (very low) to 5 (very high). In this case study a total of 16 LUs were identified, which were used to estimate a total 35 ES across three ES categories (e.g., regulating, cultural and provisioning). The following Eq. 29.3 shows the algorithm for ES capacity (ES_{Cap}) calculation as the sum of regulating (R), provisioning (P) and cultural (C) ES.

$$ES_{Cap} = R + P + C \quad (29.3)$$

Some of the past studies demonstrate the assessment of vulnerability of ecosystem services to different natural and anthropogenic hazards using variable methods. For example, Malekmohammadi and Jahanishakib (2017) assessed wetland ecosystem service vulnerability using a driver-pressure-state-impact-response model in south-western Iran; Lee et al. (2017) used storm and sea-level data to assess the vulnerability of mangrove ecosystem to climate change in Mozambique; Depellegrin et al. (2020) calculated marine ecosystem service exposure to anthropogenic threats in Lithuanian sea space using pressure propagation model and threat exposure index; and Willaert et al. (2019) assessed vulnerability of marine and coastal ecosystem services in the western Atlantic coast of Portugal using InVEST habitat risk assessment tool. A similar approach to the present research was used by Stratford et al. (2011) to assess the vulnerability of lake ecosystem services in the Himalayan area of Nepal. Stratford et al. (2011) assessed different values (i.e., ecological, economic, hydrological, social, etc.) provided by the wetland ecosystem services in the study area and considered associated threats (i.e., ecological, economic, hydrological, social, etc.) to calculate the vulnerability of ecosystem services. In this study, we used a 66 years inventory of tropical cyclone data as a threat proxy to assess the exposure of coastal ecosystem services to natural hazards in the Bangladesh coast.

In Eq. 29.4 the method of assessing ES exposure to threats cyclones is defined. We defined the threat exposure as the action of a pressure (the cyclone) on a receptor (the single or multiple ES provided; ES_{Cap}), with regards to the extent (the 20 km area of influence), magnitude (the cyclone intensity score) and the duration of the pressure (Robinson et al., 2008):

$$ES_{threat} = ES_{Cap} \times CI \quad (29.4)$$

3 Results

3.1 Ecosystem Services Capacity in the Coastal Area

Figure 29.2a presents an alluvial diagram linking the ES capacity scores from 1 (low capacity) to 5 (very high), with the LU identified in the study area (Fig. 29.1a). Results indicate that the study area has the highest ES_{Cap} for cultural ES (recreation,

landscape aesthetics and knowledge systems) and for biodiversity provision. The LU with highest ES_{Cap} are mangrove forests, hilly forests and aquatic environments (waterbodies, water courses and coastal seas). In Fig. 29.2b the geospatial results of the ES_{Cap} mapping were illustrated and in Fig. 29.2c the average contribution in % by LU to the ES_{Cap} is quantified. The overall ES_{Cap} shows that those with the highest ES capacity are located in the southern tip of the study area, in the north and inland. The LU with highest contribution to ES_{Cap} are mangrove forest (16.1%), hilly forests (14.8%), coastal sea (9.9%) with water bodies (10.5%; Fig. 29.2c). LUs with lowest ES capacity are mainly urbanized areas, such airports, port areas and developing or construction sites.

The highest contribution to ES_{Cap} for cultural ES is provided by hilly forests (12.1%), mangrove forests (12.1%), beaches (8.9%) and water courses (9.8%). Areas of highest ES_{Cap} score are located in the southern tip of the study area and in the north. In terms of provisioning ES, LUs with the highest capacity are agricultural land (12.9%) mainly for crop yield, mangrove forests (13.4%) and water bodies (14.3%). the LU of highest contribution to regulating ES are mangrove forests (22.9%), hilly forest (21.5%) and homestead vegetation (11.7%). In particular mangrove forest is the land use providing multiple ES, such as biodiversity and habitat maintenance (Brander et al., 2012), climate regulation (Peneva-Reed et al., 2020), source of wild food harvesting (Saenger et al., 2013) and sites with recreational attraction (Spalding & Parrett, 2019).

3.2 Ecosystem Services Exposure to Natural Hazard

From 1952 to 2017 the study area was hit by 34 tropical cyclones with varying intensities. Among them, some of the most devastating cyclones which caused substantial loss and damage to the lives and ES were the Bhola cyclone (1970), Urir Char cyclone (1985), Chittagong cyclone (1991), and Cyclone Mora (2017). Due to the extreme wind gust with associated storm surge, the Bhola cyclone (1970) and the Chattogram cyclone (1991) together caused 0.6 million deaths, the most devastating ever recorded (Bern et al., 1993; Frank & Husain, 1971). In the last decade deadliest tropical cyclone Mora (2017) hit the study area that caused widespread devastation and flooding in South-eastern Asia including Bangladesh, Myanmar, and East and North-east India (NOAA, 2017).

Figure 29.3 represents a workflow to assess the exposure of LU providing ES to tropical cyclones at *upazila* level. According to the cyclone intensity, as presented in Fig. 29.3a, the coastal areas most frequently hit by cyclones are located to the north of the Chattogram city covering Fatikchhari, Sitakunda, and Hathazari *upazilas*. Among 34 cyclones, 17 cyclones made landfall in this region in the last 66 years causing significant damage to the ES. Figure 29.3b shows that *upazilas* with the highest overall mean ES_{Cap} , that are located in the northern (Fatikchhari and Sitakunda) and mid-eastern (Rangunia, Chandanaish, and Lohagara) and southern (Ramu) segments of the study area. The ES threat exposure (Fig. 29.3c) reveals that

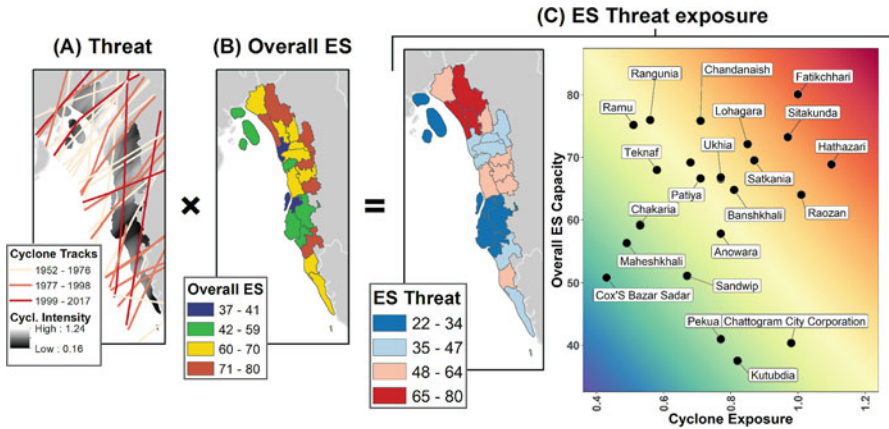


Fig. 29.3 ES threat analysis. (a) Cyclone tracks within the period 1952 to 2017 and resulting cyclone intensity; (b) mean overall ES_{Cap} at *upazila* level and (c) resulting ES threat exposure map and a 2D plot comparing ES_{Cap} with cyclone exposure

ES provision is most threatened by cyclones in the *upazilas* located in the northern part of the study area, while coastal *upazilas* situated in the central and the south show comparatively lower impacts. The 2D plot comparing the overall ES_{Cap} with cyclone exposure gradient represents the *upazilas* named Fatikchhari, Sitakunda and Hathazari belong to the most threatened sites with comparably higher overall ES_{Cap} (Fig. 29.3c). In contrast, *upazilas* like Kutubdia, Pekua, Sandwip, Maheshkhali, Cox’s Bazar Sadar, and Chattoogram City have a low ES_{Cap} with comparably lower cyclone exposure. This plot concludes that all the higher ES provisioning administrative units fall in the with higher exposure to tropical cyclones in the eastern coast of Bangladesh.

4 Discussion and Conclusion

Bangladesh is a multi-disaster-prone country in South Asia. Being exposed to the Bay of Bengal, the southern coastal region of the country is vulnerable to numerous anthropogenic and natural hazards. Current century climate change has been posing a severe threat to the coastal habitats and livelihood by accelerating other hazards such as sea-level rise, salinity intrusion, tidal flooding, tropical cyclones, and associated storm surges. Apart from these changing land uses, unregulated mass tourism, unplanned emergence of economic activities, coastal water pollution, and acidification has been exerting tremendous pressures on the coastal ecosystems. Over the last decades, several policies and strategies have been adopted at the national level aiming to reduce exposure of the coastal region to different natural hazards. The major policies/strategies considering the reduction of coastal region’s

vulnerability to coastal hazards and increasing resilience include National Development Strategy (2010–2021), Environmental Policy (1992), Coastal Zone Policy (2005), Coastal Development Strategy (2006), National Fisheries Policy (1998), National Adaptation Program of Action (NAPA), Bangladesh Climate Change Strategy and Action Plan (2009), National Plan for Disaster Management (2010–2015), and Bangladesh Delta Plan-2100. Most of these policies and strategies focused on building the resilience of the coastal communities to natural hazards, while few strategies considered infrastructural development and establishing coastal green belt through planting mangroves for the protection of coastal ecosystems and livelihoods during disaster events. Since 1966 several afforestation and reforestation projects have been implemented in the coastal and offshore regions of the country for protecting coastal communities from cyclone and storm surges. Subsequent to the 1991 Chittagong Cyclone, a number of multi-purpose cyclone shelters were established throughout the coastal area under government and private sector investments, which significantly reduced loss of lives and economic properties during the cyclones of the following years. Despite Bangladesh has an improved disaster management framework, the existing initiatives are still inadequate to provide protection to the coastal ecosystem services from particular hazards such as cyclones. Furthermore, the lack of appropriate regulation and monitoring for coastal land uses and their transition to other uses, respectively, have been deteriorating coastal habitat quality and ecosystem functioning. Though some of the uses proving people more economic benefit, these are degrading environment for the long term on the other hand. For example, sea salt production and shrimp farming at the Maheshkhali area are economically profitable but these land uses are environmentally unsustainable due to their uncontrolled practices.

The presented research shows how the integration of ecosystem services knowledge can be flexibly incorporated into disaster risk assessment from tropical cyclones. It shows the areas having the potentials of providing different ES and their gradient of exposure to the most dominant hazard, tropical cyclone, in the eastern coastal region of the country.

The geospatial distribution of the ES and threat scores together can inform the policymakers which areas are high potentials for getting benefit and how to protect them from cyclone hazard. Considering that according to our study about 3723 km² (52%) of the study area belongs to green infrastructure such as mangroves, hilly forests and tidal flats that provide high to very high protection from natural hazards. The findings can be used for developing sustainable land use plans for the coastal region, which together can provide sufficient ES provision to support human well-being, livelihoods and increase environmental security.

This presented approach is not free of limitations. In this research to estimate ES, we considered dominant land uses practiced in the area. There are certainly other uses with ES potentials that should be considered in the assessment stage. Moreover, the modelled cyclone intensity considered a 20 km buffered cyclone track as the high impact area. But the impact area of different cyclones can be variable. Moreover, the storm surge accompanied by cyclonic events, which causes secondary damage to the coastal ES, is overlooked in our approach.

The ES indicators used in this research should be further extended by incorporating the quantitative indicators (e.g., economic values) for ES services flow and demand. In particular, this is important for the quantification of damages on ES supporting livelihoods, agricultural yield, clean water, irrigation, and cultural well-being. ES can act as a green infrastructure and provide protection services from cyclones. LUs that are particularly important for natural hazard protection are mangrove forests and hilly forests. Attention should be given to coastal planning and land use management practices that ensure natural protection from natural hazards.

Acknowledgement We sincerely acknowledge Central Library of the University of Dhaka, Bangladesh for providing access to the national newspaper archive. We are also thankful to the USGS EROS data center and IBTrACS for providing satellite imagery and cyclone tracks, respectively for the study area. Daniel Depellegrin was funded by the PostDoc Grant of the University of Girona 2021 “Sum of Intelligences” (Contract Number: 420).

References

- Alam, E., & Dominey-Howes, D. (2014). A new catalogue of tropical cyclones of the northern Bay of Bengal and the distribution and effects of selected landfalling events in Bangladesh. *International Journal of Climatology*, 35(6), 801–835. <https://doi.org/10.1002/joc.4035>
- BBS. (2011). *Population and housing census*. Bangladesh Bureau of Statistics. Ministry of Planning. Government of the People’s Republic of Bangladesh.
- Bern, C., et al. (1993). Risk factors for mortality in the Bangladesh cyclone of 1991. *Bulletin of the World Health Organization*, 71(1), 73–78. Available at: <https://apps.who.int/iris/handle/10665/49886>. Accessed 12 Jan 2021
- BMD. (2013). Bangladesh Meteorological Department, Annual rainfall and temperature analysis. <http://www.bmd.gov.bd/>. Accessed 29 Dec 2020.
- Brander, L. M., Wagtendonk, A. J., Hussain, S., McVittie, A., Verburg, P. H., de Groot, R. S., & van der Ploeg, S. (2012). Ecosystem service values for mangroves in Southeast Asia: A meta-analysis and value transfer application. *Ecosystem Services*, 1, 62–69. <https://doi.org/10.1016/j.ecoser.2012.06.003>
- Burkhard, B., Kroll, F., Müller, F., & Windhorst, W. (2009). Landscapes’ capacities to provide ecosystem services – A concept for land-cover based assessments. *Landscape Online*, 15, 1–22. <https://doi.org/10.3097/lo.200915>
- Campagne, C. S., Roche, P., Müller, F., & Burkhard, B. (2020). Ten years of ecosystem services matrix: Review of a (r)evolution. *One Ecosystem*, 5, e51103. <https://doi.org/10.3897/oneeco.5.e51103>
- Depellegrin, D., Menegon, S., Farella, G., Ghezzi, M., Gissi, E., Sarretta, A., Venier, C., & Barbanti, A. (2017). Multi-objective spatial tools to inform maritime spatial planning in the Adriatic Sea. *Science of the Total Environment*, 609, 1627–1639. <https://doi.org/10.1016/j.scitotenv.2017.07.264>
- Depellegrin, D., Menegon, S., Gusatu, L., Roy, S., & Misiunè, I. (2020). Assessing marine ecosystem services richness and exposure to anthropogenic threats in small sea areas: A case study for the Lithuanian Sea space. *Ecological Indicators*, 108, 105730. <https://doi.org/10.1016/j.ecolind.2019.105730>
- Emran, A., Roy, S., Bagmar, M. S. H., & Mitra, C. (2018). Assessing topographic controls on vegetation characteristics in Chittagong Hill Tracts (CHT) from remotely sensed data. *Remote*

- Sensing Applications: Society and Environment*, 11, 198–208. <https://doi.org/10.1016/j.rsase.2018.07.005>
- FLAASH User's Guide. (2006). *FLAASH module user's guide, FLAASH module version 4.3*. ITT Visual Information Solutions. https://popo.jpl.nasa.gov/pub/ENVI_Installers/ENVI_Documentation/docs/FLAASH_Module.pdf. Accessed 26 Feb 2021.
- Frank, N. L., & Husain, S. A. (1971). The deadliest tropical cyclone in history. *Bulletin of the American Meteorological Society*, 52(6), 438–445. [https://doi.org/10.1175/1520-0477\(1971\)052<0438:tdtcih>2.0.co;2](https://doi.org/10.1175/1520-0477(1971)052<0438:tdtcih>2.0.co;2)
- Hoque, M. A. A., Pradhan, B., Ahmed, N., & Roy, S. (2019). Tropical cyclone risk assessment using geospatial techniques for the eastern coastal region of Bangladesh. *Science of the Total Environment*, 692, 10–22. <https://doi.org/10.1016/j.scitotenv.2019.07.132>
- Kaiser, G., Burkhard, B., Römer, H., Sangkaew, S., Graterol, R., Haitook, T., Sterr, H., & Sakuna, D. (2013). Mapping tsunami impacts on land cover and related ecosystem service supply in Phang Nga, Thailand. *Natural Hazards and Earth System Sciences*, 13, 3095–3111. <https://doi.org/10.5194/nhess-13-3095-2013>
- Lee, C. K. F., Duncan, C., Owen, H. J. F., & Pettorelli, N. (2017). A new framework to assess relative ecosystem vulnerability to climate change. *Conservation Letters*, 11(2). <https://doi.org/10.1111/conl.12372>
- Malekmohammadi, B., & Jahanishakib, F. (2017). Vulnerability assessment of wetland landscape ecosystem services using driver-pressure-state-impact-response (DPSIR) model. *Ecological Indicators*, 82, 293–303. <https://doi.org/10.1016/j.ecolind.2017.06.060>
- Meixler, M. (2017). Assessment of Hurricane Sandy damage and resulting loss in ecosystem services in a coastal-urban setting. *Ecosystem Services*, 24, 28–46. <https://doi.org/10.1016/j.ecoser.2016.12.009>
- Müller, F., Bicking, S., Ahrendt, K., Kinh Bac, D., Blindow, I., Fürst, C., Haase, P., Kruse, M., Kruse, T., Ma, L., Perennes, M., Ruljevic, I., Schemewski, G., Schimming, C.-G., Schneiders, A., Schubert, H., Schumacher, N. J., Tappeiner, U., Wangai, P., ... Zeleny, J. (2020). Assessing ecosystem service potentials to evaluate terrestrial, coastal and marine ecosystem types in Northern Germany – An expert-based matrix approach. *Ecological Indicators*, 112, 106116. <https://doi.org/10.1016/j.ecolind.2020.106116>
- NOAA. (2017). *Cyclone Mora hits vulnerable Bangladesh*. <https://www.climate.gov/news-features/event-tracker/cyclone-morahits-vulnerable-bangladesh>. Accessed 19 April 2022.
- Peneva-Reed, E. I., Krauss, K. W., Bullock, E. L., Zhu, Z., Woltz, V. L., Drexler, J. Z., Conrad, J. R., & Stehman, S. V. (2020). Carbon stock losses and recovery observed for a mangrove ecosystem following a major hurricane in Southwest Florida. *Estuarine, Coastal and Shelf Science*, 106750. <https://doi.org/10.1016/j.ecss.2020.106750>
- Robinson, L. A., Rogers, S., & Frid, C. L. J. (2008). A marine assessment and monitoring framework for application by UKMMAS and OSPAR - Assessment of Pressures and Impacts. *Phase II: Application for regional assessments*. JNCC Contract No: C-08-0007-0027. UKMMAS, 2010. Charting Progress 2.
- Roy, S., & Mahmood, R. (2016). Monitoring shoreline dynamics using Landsat and hydrological data: A case study of Sandwip Island of Bangladesh. *Pennsylvania Geographer*, 54(2), 20–41.
- Roy, S., Pandit, S., Eva, E. A., Bagmar, M. S. H., Papia, M., Banik, L., Dube, T., Rahman, F., & Razi, M. A. (2020). Examining the nexus between land surface temperature and urban growth in Chattogram Metropolitan Area of Bangladesh using long term Landsat series data. *Urban Climate*, 32, 100593. <https://doi.org/10.1016/j.uclim.2020.100593>
- Saenger, P., Gartside, D., & Funge-Smith, S. (2013). *A review of mangrove and seagrass ecosystems and their linkage to fisheries and fisheries management* (RAP PUBLICATION 2013/09). FAO Regional Office for Asia and the Pacific. Food and Agriculture Organization of the United Nations Regional Office for Asia and the Pacific. ISBN:978-92-5-107773-3.
- Spalding, M., & Parrett, C. L. (2019). Global patterns in mangrove recreation and tourism. *Marine Policy*, 110, 103540. <https://doi.org/10.1016/j.marpol.2019.103540>

- Stratford, C. J., Acreman, M. C., & Gwyn Rees, H. (2011). A simple method for assessing the vulnerability of wetland ecosystem services. *Hydrological Sciences Journal*, 56(8), 1485–1500. <https://doi.org/10.1080/02626667.2011.630669>
- USGS. (2020). *Using the USGS Landsat level-1 data product, Landsat missions*. <https://www.usgs.gov/core-science-systems/nli/landsat/using-usgs-landsat-level-1-data-product>. Accessed 29 Dec 2020.
- Villamagna, A. M., Angermeier, P. L., & Bennett, E. M. (2013). Capacity, pressure, demand, and flow: A conceptual framework for analyzing ecosystem service provision and delivery. *Ecological Complexity*, 15, 114–121. <https://doi.org/10.1016/j.ecocom.2013.07.004>
- Williaert, T., García-Alegre, A., Queiroga, H., Cunha-e-Sá, M. A., & Lillebø, A. I. (2019). Measuring vulnerability of marine and coastal habitats' potential to deliver ecosystem services: Complex Atlantic region as case study. *Frontiers in Marine Science*, 6, 199. <https://doi.org/10.3389/fmars.2019.00199>

Open Access This chapter is licensed under the terms of the Creative Commons Attribution 4.0 International License (<http://creativecommons.org/licenses/by/4.0/>), which permits use, sharing, adaptation, distribution and reproduction in any medium or format, as long as you give appropriate credit to the original author(s) and the source, provide a link to the Creative Commons license and indicate if changes were made.

The images or other third party material in this chapter are included in the chapter's Creative Commons license, unless indicated otherwise in a credit line to the material. If material is not included in the chapter's Creative Commons license and your intended use is not permitted by statutory regulation or exceeds the permitted use, you will need to obtain permission directly from the copyright holder.

